Surface Science 268 (1992) 142–154
North-Holland

surface science

Effect of strain on thin film growth: deposition of Ni on Ag(100)

Barry C. Bolding and Emily A. Carter
Department of Chemistry and Biochemistry, University of California, Los Angeles, CA 90024-1569, USA

Received 10 September 1991; accepted for publication 4 December 1991

The results of Monte Carlo simulations of the structure and energetics of Ni thin films grown on Ag(100) are discussed. Despite a 13.9% lattice mismatch, layer-by-layer growth of pseudomorphic Ni is favored over an incommensurate Ni(111) structure, up to approximately ~ 3.2 ML Ni. Reconstruction or clustering of the Ni overlayer is seen at submonolayer to monolayer coverages. The pseudomorphic multilayer film has a tetragonal structure due to the expansive intralayer strain inducing a compressive interlayer stress. The tetragonal Ni(100) overlayer appears metastable, since allowing interdiffusion via exchange of Ni and Ag atoms leads to a thermodynamically favored Ag/Ni/Ag(100) sandwich structure. A buckled, close-packed Ni(111) thin film structure is preferred at higher coverages and is found to inhibit interdiffusion of Ag atoms. A direct commensurate–incommensurate phase transition is never observed.

1. Introduction

Understanding the effect of substrate-induced lattice strain on thin film structures has been an active area of research for many years [1–4]. Both interfacial and intralayer strain influence the structure of the growing thin film, producing several possible adlayer structures: (i) a phase in which the film adopts the same lattice as the substrate (i.e., pseudomorphic); (ii) a phase with periodic misfit-induced defects in the thin film structure (with pseudomorphic or commensurate regions between defects); (iii) a phase that is different from both the substrate and the adlayer preferred bulk structures (e.g., a commensurate reconstruction); or (iv) a phase where the adlayer forms its preferred bulk structure, independent of the underlying substrate structure (i.e., incommensurate). The structure of the thin film is extremely important to elucidate, since it is expected to dictate the physical and chemical characteristics of the film, such as its magnetic properties, binding energies of molecules at the gas/thin film interface, and electronic properties (due to an altered band structure).

A great deal of theoretical work has been devoted. to understanding the conditions for pseudomorphic and misfit film growth. Pioneering studies by Frank, van der Merwe, and Bauer and co-workers [1,3–5], employed classical, continuum models of rigid substrates and adlayers. These models predicted pseudomorphic growth can occur for lattice mismatches between the substrate and adlayer (i.e., strains) of up to 9%. More recently, Markov and Milchev [6–8] have used a numerical solution of the anharmonic Toda potential to model epitaxial interfaces. In contrast to the continuum models, they predicted an upper limit of ~ 13.5% lattice mismatch for pseudomorphic growth of one-dimensional epitaxial films.

Dodson and Taylor [9,10] examined two-dimensional heteroepitaxy using a Lennard-Jones potential and molecular dynamics (MD) and Monte Carlo (MC) methods. These two-dimensional systems show pseudomorphic growth for lattice strains less than 4% and defective growth at higher lattice strain. Using a similar potential and performing discrete-space MC simulations, Faux et al. [11] varied the degree of lattice strain

in two-dimensional films and found widely varying growth modes in the 1–10% lattice strain range. In agreement with Dodson and Taylor, pseudomorphic growth was predicted only for strains less than 4%. Layer-by-layer (Frank–van der Merwe) growth was found for mismatches of up to 2%, while three-dimensional (Volmer–Weber) growth was predicted for larger lattice mismatches.

Static energy studies of strained metal films have been examined by Dodson [12] and by Kobayashi and Das Sarma [13]. Employing the same type of interaction potentials used in the present study, Dodson predicted that pseudomorphic growth should occur for films with less than 7–10% lattice strain, with growth under such strain conditions predicted to be most favorable when an element with a larger atomic radius is deposited on a substrate with smaller atomic radius. Kobayashi and Das Sarma [13] have used rigid adlayer–substrate models to show that the energetics of thin film growth depends on complicated contributions from the ratios of the atomic radii of the substrate and adlayer, as well as the ratios of the relevant interaction energies.

Several studies have been performed with the goal of modeling specific real materials containing lattice strain. Nandedkar et al. [14] have performed 0 K Lennard-Jones potential studies of Au(111)/Ni(111) and Au(100)/Ni(100), which have a 15.9% mismatch, in order to determine the formation and structure of misfit dislocations. They found that misfit dislocations were readily created upon energy minimisation. Murthy and Rice [15] investigated the energetics of monolayers with small lattice strain using both the embedded-atom method (EAM) and simple pair potentials to describe Cu on Ni(100). They predicted that the negative misfit system [16] (Ni on Cu) has more of a tendency to grow pseudomorphically than the positive misfit system (Cu on Ni), contrary to Dodson's general predictions [12]. By varying the magnitude of the adatom–adatom interaction energy, they concluded that the thin film structure is very sensitive to the adatom–adatom interaction and that this must be modeled accurately to correctly model thin film growth. Thus previous studies that considered only the substrate–adatom interaction and adatom–adatom interactions via the elastic properties of the layer [1,3–8,13,17] are limited in their usefulness. The formation of surface alloys of Au on Cu(100) has been investigated by Foiles using the EAM potential [18]. A surface $c(2 \times 2)$ alloy was found to be stable, in agreement with experiment. The structure and dynamics of several heteroepitaxial systems have also been studied by Raeker et al. [19,20] using the corrected effective medium potential. A wide variety of phenomena were predicted, including "sandwich" formation for Rh on Ag(100) and surface alloy formation for Au on Cu(100), in agreement with Foiles [18].

We have recently examined [21,22] structures formed as a function of temperature and coverage for an fcc metal (Pd) deposited on a bcc(110) substrate (e.g., Ta or Nb). The large lattice mismatch in this system (18% in one direction, 2% in the orthogonal direction), as well as the difference in preferred bulk structures (fcc versus bcc) leads to a commensurate–incommensurate (C–I) phase transition at high temperatures for coverages above 1.0 bcc monolayers (ML). The work described herein is for a system again with large lattice mismatch (13.9%), but with two metals that have the same preferred bulk configuration (namely fcc). This study is meant to provide a contrast or a control by examining only one variable this time, i.e., lattice mismatch in the absence of the fcc–bcc asymmetry present in our first set of studies.

In particular, we present results-for a simulation of Ni grown on Ag(100), as representative of a class of fcc/fcc(100) interfacial materials. Our interest in Ag/Ni interfaces was prompted by several unusual observations of both their geometrical and electronic properties. For example, growth of Ag on Ni(100) is characterized by a $c(2 \times 8)$ low energy electron diffraction (LEED) pattern, which has been interpreted in terms of a distorted hexagonal overlayer [23]. It appears that the much larger Ag atoms have no inclination to grow pseudomorphically on the smaller Ni substrate. Ag/Ni superlattices exhibit novel variations in the magnetization of the Ni layers as a function of film thickness [24,25]. Finally, the

upward migration of atoms from the substrate to form a single capping layer over the thin film has been observed experimentally for many bimetallic systems, including Rh grown on Ag(100) [26] and Cu(100) [27], as well as for Ag/Ni bilayers [28]. This effect has also been confirmed by simulations for the Rh/Ag(100) system [19].

As the above review of past theoretical work suggests, simple models which differ in their physical assumptions (e.g., rigid substrate or adlayer, neglect of interactions within the adlayer, two-dimensional systems, etc.) yield a wide range of predictions about the type of growth and structure of the thin film. Hence our study reported here has attempted to model the fcc on fcc(100) system as realistically as possible, by doing away with assumptions of rigid interfaces and neglect of certain interactions. The model potential and theoretical techniques employed are discussed in the next section. Results are presented in section 3, with a summary and conclusions given in section 4.

2. Method

In order to model the Ni/Ag(100) system, we have chosen to use the embedded-atom potential energy functions developed by Foiles, Baskes, and Daw [29]. This model has been tested extensively on bulk, alloy and interfacial systems [29–31]. Some examples of the use of the EAM potential include studies of the critical thickness of thin fcc(111)/fcc(111) films by Dodson [12], examination of the elastic properties of thin slabs by Wolf [33], relaxation at the Ni(110)/Ag(110) interface [34] and recent work by the present authors studying structural properties of fcc/bcc interfaces [21,22]. The results of these studies substantiate the use of the EAM potential for thin films.

The periodic simulation cell size was taken to be an integer multiple of the substrate Ag(100) square unit cell ($a_0 = 4.09$ Å) and as close as possible to an integer multiple of both the Ni(100) and Ni(111) surface unit cells. An optimal value was found to be 17 lattice units long (69.53 Å) in the [010] and 6 lattice units long (24.54 Å) in the [001] direction, resulting in 204 Ag atoms/layer. These dimensions minimize any lateral strain if either a perfect Ni(111) (with Ni $[01\bar{1}]$ parallel to Ag [001]) or a perfect Ni(100) adlayer were to form. Additional simulations were performed with 19×19 and 38×6 Ag(100) substrates, which minimize the boundary induced strain in the Ni(111) adlayers. For most of the simulations, the substrate was modeled with two movable Ag layers at the interface and three fixed Ag layers below the other two, although some calculations were performed with one movable and four fixed layers or three movable and three fixed Ag layers.

Monte Carlo simulations were used both to deposit and to equilibrate Ni atoms into the thin film, as well as to equilibrate the movable substrate atoms. To model deposition of the Ni film, we choose a random x and y position in the periodic cell (parallel to the surface). The z (surface normal) position of the new adatom was chosen to be 2.0 ± 0.3 Å above the topmost Ni layer in the growing film, with the actual value chosen randomly within this range. A Ni atom was deposited every 50 000–400 000 MC equilibration steps. A variable maximum random displacement was used, which maintained the acceptance ratio close to 0.33 for both the substrate and adlayer atoms. At specific coverages (0.93, 1.37, 1.56, 2.00, 3.13 and 3.43 ML, where ML is the number of substrate equivalent monolayers), extensive simulations involving 5–20 million MC steps were performed in order to equilibrate the adlayer. Most of the deposition studies were performed at a temperature of 300 K, although we also simulated some heating and cooling to investigate changes in the structure of the film with temperature.

Once the structure was equilibrated at each of these coverages (0.93, 1.37, 1.56, 2.00, 3.13 and 3.43 ML), several different probes were used to characterize the structure of the films. First, both radial and angular distribution functions, $g(r)$ and $g(\theta)$, were analyzed for all atoms in each layer of the film and substrate. The angular distribution function, $g(\theta)$, was constructed by finding all neighbors of each atom within a radial cutoff of 3.50 Å (the usual position of the mini-

mum between the first and second peaks in the $g(r)$, i.e. a distance between the nearest and next-nearest neighbors). Then all of the angles between these atoms are calculated, normalized by the total number of atoms in the adlayer. Our standard point of reference, the perfect Ag(100) substrate, exhibits a radial distribution with a nearest-neighbor(nn) peak at 2.89 Å and next-nearest-neighbor(nnn) peak at 4.09 Å. The angular distribution has peaks at 90 and 180 degrees. By contrast, the perfect Ni(111) adlayer (with $a_0 = 3.52$ Å) exhibits radial distribution peaks at 2.49 Å (nn) and 4.31 Å (nnn) and angular distribution peaks at 60, 120 and 180 degrees. A Ni(100) adlayer will have a similar $g(\theta)$ to Ag(100) of course, but the perfect Ni(100) $g(r)$ will have a nn peak at 2.49 Å and a nnn peak at 3.52 Å. Thus all three idealized adlayer structures will be readily identifiable and distinguishable by a combination of $g(r)$ and $g(\theta)$. Secondly, bond diagrams were used to visualize the structures formed during thin film growth. This involved drawing the atoms within a given Ni layer and sketching a bond between them if they are within a given radial cutoff (typically between 2.8 to 3.5 Å) of each other. This helps to determine which Ni atoms are forming contracted and/or expanded bonds.

3. Results and discussion

3.1. Zero coverage adsorption of Ni on Ag(100)

We first investigated the adsorption of a single Ni atom on a rigid Ag(100) substrate by energy minimization. Ni was found to bind most strongly in the pseudomorphic positions with a binding energy of 3.24 eV, substantially lower than the bulk Ni cohesive energy predicted with the EAM potential (4.45 eV for both experiment and theory). The barriers to diffusion were found to be 1.11 eV over an atop site and 0.62 eV over a two-fold bridging site, with saddle point coordinates of 1.74 and 1.42 Å, above the plane of the Ag substrate, respectively. In its equilibrium pseudomorphic position, the nickel atom is found to rest only 1.00 Å above the plane of the top Ag(100) layer. Unfortunately, no experimental data from LEED, field ion microscopy, ion scattering spectroscopy (ISS) [35] or surface extended

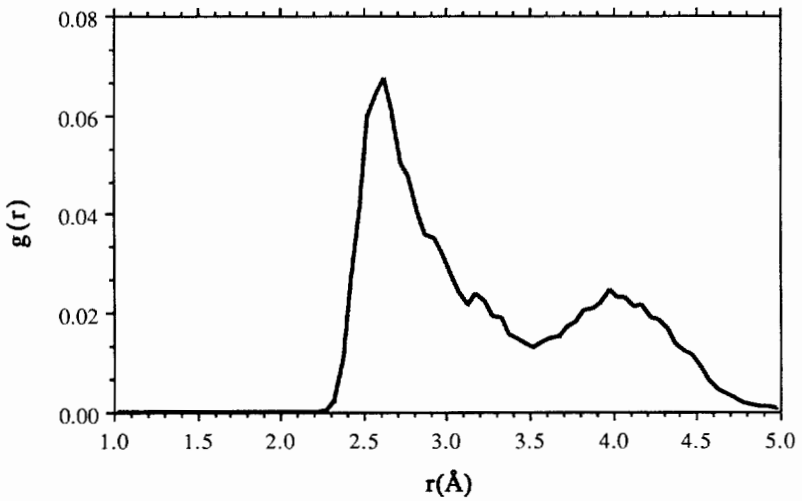

Fig. 1. The Ni–Ni radial distribution function, $g(r)$, for a 1.0 ML coverage of Ni/Ag(100). The nearest-neighbor(nn) peak is broad with a single maximum at 2.63 Å, which represents a contraction of the Ni–Ni bonds from the ideal pseudomorphic length of 2.89 Å.

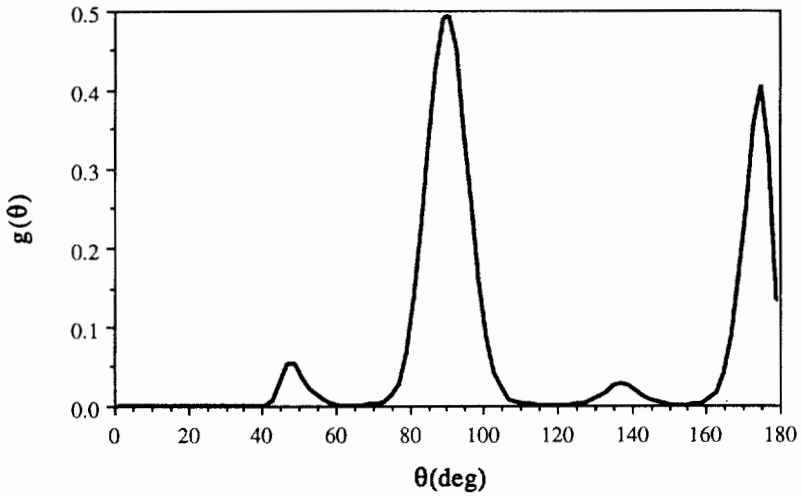

Fig. 2. The angular distribution function, $g(\theta)$, for a 1.0 ML coverage of Ni/Ag(100). The primary peaks at 90° and 176° are characteristic of the square (100) surface.

X-ray absorption fine structure (SEXAFS) is yet available with which to compare.

3.2. Submonolayer to monolayer coverage of Ni on Ag(100)

Random deposition of Ni atoms onto a Ag(100) substrate at 300 K yields initial thin film growth of Ni that is roughly pseudomorphic with the substrate. The submonolayer up to monolayer structure of the Ni thin film is distinguished by a broad first peak in the Ni–Ni radial distribution function (fig. 1) with a maximum at 2.63 Å. This lies between the bulk Ni–Ni near neighbor distance of 2.49 Å and the Ag–Ag near neighbor distance of 2.89 Å. If the thin Ni film was forming a structure similar to Ni(111), then a strong second neighbor peak in the $g(r)$ would be present at 4.31 Å and the angular distribution would have peaks at 60°, 120° and 180°. If the Ni film was forming a Ni(100) structure, it would have a nnn peak in the $g(r)$ at 3.52 Å and angular distribution peaks at 90° and 180°. The angular distribution function is indicative of a square lattice

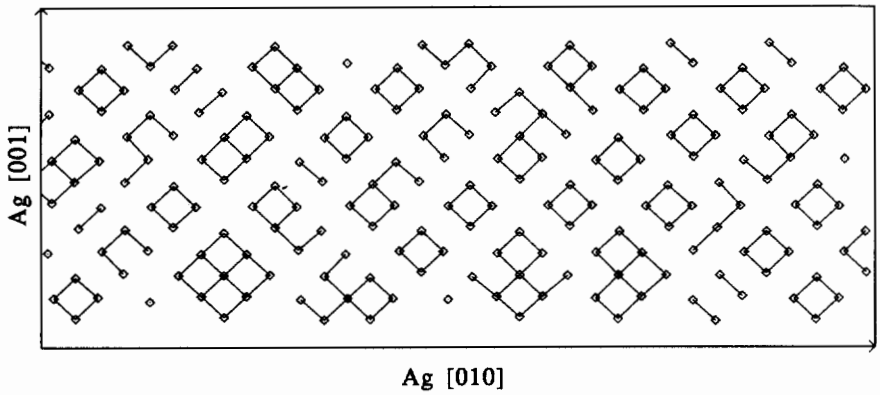

Fig. 3. A bond diagram for 1.0 ML of Ni on Ag(100) that has been quenched to 0 K. Atoms are shown as squares and a bond is drawn between atoms less than 2.8 Å apart. Substrate atoms are not shown. The local contraction of the Ni–Ni NN distance and formation of small clusters is evident.

because of the large peaks at 90° and near 180° (fig. 2). However, the nnn peak in the radial distribution function is at 4.0 Å, which is farther out than the Ni(100) nnn peak but close to the Ag(100) nnn peak. These two facts suggest that the Ni film is growing pseudomorphic with the underlying Ag(100) structure but with considerable distortion of the lattice. The Ni–Ni nn distance is smaller than the Ag–Ag nn distance expected for the pseudomorphic structure because of formation of small groups of Ni atoms that contract toward one another while staying in the pseudomorphic lattice wells. This is illustrated by the bond diagram structure shown in fig. 3, where bonds have been drawn between atoms that are less than 2.80 Å apart. This cutoff at 2.80 Å is arbitrary and has no relation to the true metallic bonding, but allows us to distinguish between bulk-like Ni–Ni bonds and highly stretched Ni–Ni bonds with bond lengths close to those of Ag. This structure shown in fig. 3 is for a 1.0 ML film that has been quenched to 0 K. The small groups of 4–8 adatoms each nevertheless maintain registry with the substrate but have bro-

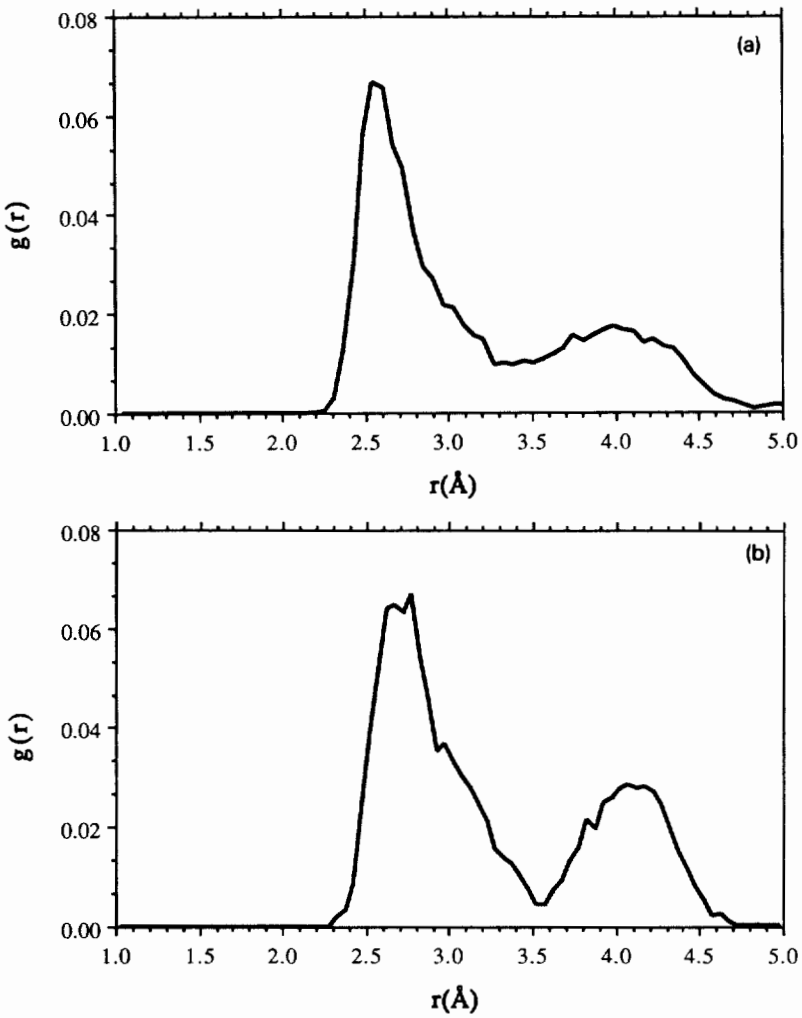

Fig. 4. The radial distribution function for (a) the second Ni layer forming at $\Theta_{Ni} = 1.5$ ML and (b) the first pseudomorphic Ni layer (closest to the substrate) for $\Theta_{Ni} = 2.0$ ML. The NN peak now has a broad maximum between 2.62 and 2.75 Å.

ken its symmetry. Such a structure might be observed in LEED, exhibiting a larger unit cell (e.g., 2×1 or 2×2) than the substrate.

3.3. Ni multilayers on Ag(100)

The Ni film continues to grow pseudomorphically up to $\Theta = 4.2$ ML by room temperature deposition. (Films thicker than 4.2 ML were not examined by deposition.) The film grows roughly layer-by-layer, although a new layer always starts to grow before the previous layer is completely filled. Structural changes as a function of coverage are primarily evident in the Ni–Ni radial distribution function, where the position of the first maximum shifts outward with coverage. As the second layer initially forms (1.0–1.5 ML; fig. 4a) the first peak in the Ni–Ni $g(r)$ for the second layer atoms has a sharp maximum at 2.57 Å. This gradually shifts toward a broader nn peak at 2.62–2.75 Å as the coverage increases to 2.0 ML (see fig. 4b). Thus, when a layer is less than half completed, we observe some clustering occurring, as evidenced by bond length contractions in the $g(r)$. The clustering disappears as the layer fills completely. The broadening in the $g(r)$ for a more than half-completed layer is due to a few Ni atoms that reside in third layer positions and that subsequently induce some bonds in the second layer to lengthen. The layer of nickel closest to the substrate also undergoes a shift of the first neighbor peak from 2.57 Å ($\Theta_{Ni} < 1.0$ ML) to 2.75 Å ($\Theta_{Ni} = 2.0$ ML). Fig. 5 displays the radial distribution functions for the first and fourth Ni layers at a coverage of 4.2 ML. The graph clearly shows that the first Ni layer (closest to the Ag substrate) has a maximum at 2.80 Å, while the fourth Ni layer has a primary peak at 2.60 Å. Thus, at the interface, the Ni atoms attempt to relieve interfacial strain by adopting an Ag-like nn distance, while farther away from the interface, the nn distance contracts to relieve intralayer strain. Indeed, the average nn distances decrease monotonically away from the interface: 2.80 Å for the first layer, 2.68 Å for the second layer, 2.63 Å for the third and fourth layers, and 2.48 Å for the few atoms in the fifth layer. The interlayer Ni–Ni nn distance is found to be 2.43 Å, close to that for bulk Ni (2.49 Å). However, the interlayer spacing in the normal direction is only 1.30 Å, compared to 1.76 Å for the (100) surface of bulk Ni. Thus, pseudomorphic growth induces the interlayer Ni–Ni spacing to contract, in order to compensate for the isotropic expansive strain within each Ni adlayer (see fig. 6). The Ni film has thus assumed a tetragonal phase in

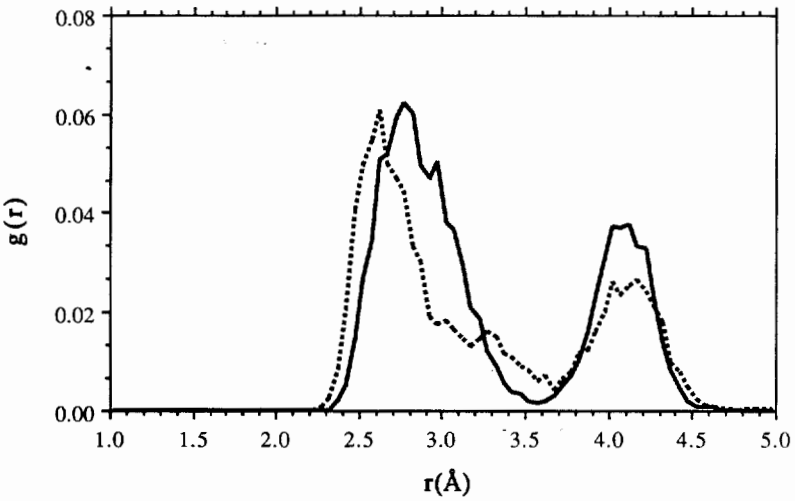

Fig. 5. The first and fourth Ni layers in a 4.2 ML thin film. The first layer is closest to the substrate (solid line) and has expanded so that the NN bond length is much closer to that of the substrate. The fourth layer (dashed line) NN bond length is contracted to 2.60 ML, much like the 1 ML $g(r)$ of fig. 1.

which the two of the lattice dimensions are 4.09 Å and the third is ~2.60 Å.

To summarize, the film grows as follows: (i) a pseudomorphic Ni layer begins to form in which the bonds parallel to the surface are contracted (from the ideal pseudomorphic length) to form 4–8 atom clusters; (ii) as the previous layer of Ni is completed, the next layer begins to form, causing the parallel nn distribution to broaden for the previous layer (2.62–2.75 Å) and to be contracted for the newly forming layer; and (iii) as several layers build up,the Ni atoms closest to the interface become pinned to pseudomorphic sites and their nn distribution again becomes sharp (at 2.80 Å). Thus, the Ni atoms closest to the interface are under the largest expansive strain, with the strain diminishing away from the interface. Interestingly, the fourth layer of Ni is still perturbed by the substrate, since the nn bond lengths parallel to the substrate are still stretched by ~0.1 Å relative to bulk Ni. Since the interlayer spacing is severely contracted from that of bulk Ni, the final multilayer structure can be considered a tetragonal phase of Ni.

3.4. Idealized adlayer structures

In order to further investigate the stability of these thin films, we studied the 0 K energetics of various structures. For our periodic boundary conditions, one atomic layer of Ni(111) is composed of 320 Ni atoms. We quenched such a structure to 0 K atop both a rigid and a relaxed Ag(100) substrate (two layers of Ag were allowed to relax). We then compared this Ni(111) energy to that of 320 pseudomorphic Ni atoms (1.56 ML) and to 320 Ni(110) atoms (189 in the first layer and 131 atoms in the second layer) quenched to 0 K. We performed the same procedure for two and three layers of Ni(111). Relaxation of the Ag

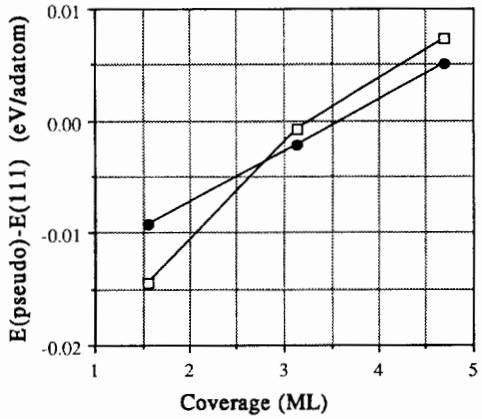

Fig. 7. Difference in the internal energies of the pseudomorphic Ni and Ni(111) thin films as a function of coverage at 0 K. The energy difference for both an unrelaxed (squares) and a relaxed (circles) Ag(100) substrate are shown.

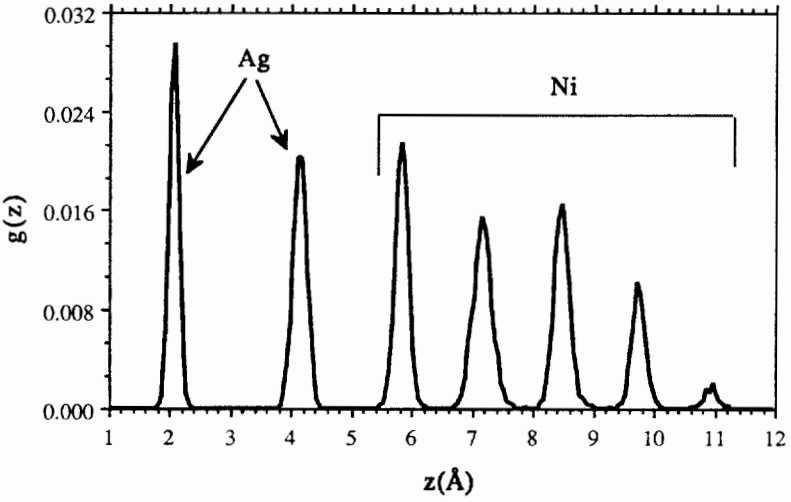

Fig. 6. The $g(z)$ atomic distribution (normal to the surface) at 300 K for a coverage of 4.2 ML. The fixed Ag substrate layers are not shown. The Ni–Ni interlayer spacing contracts to 1.30 from 1.76 Å in bulk Ni.

layers had a minimal effect on the energetics (see fig. 7). For 320 atoms, we find the pseudomorphic film more stable than the Ni(111) film by ~ 0.009 eV/adatom. The Ni(110) structure is found to be unstable and transforms to a pseudomorphic structure upon quenching. For 640 Ni atoms (3.13 ML), the pseudomorphic film is still the most stable, but now by only ~ 0.002 eV/adatom compared to a Ni(111) film. Finally for 960 Ni atoms (4.70 ML), the Ni(111) structure is found to be more stable by ~ 0.005 eV/adatom. The energy differences between the Ni(111) and pseudomorphic structures (fig. 7) suggest that at 0 K, a phase transition from a commensurate to incommensurate film is thermodynamically favorable at a coverage between 3.3 and 3.6 ML of Ni. However, differences in the heat capacities of the two structures could alter this prediction at finite temperatures.

Although we find that the Ni(111)/Ag(100) interface becomes thermodynamically favored for $\Theta_{Ni} \approx 3.5$ ML, a metastable pseudomorphic phase may form instead because of the large energy barrier required to effect the collective motions necessary for a phase transition. This kinetic limitation is most prevalent at low temperatures, where insufficient energy is available to induce the phase transformation. We have studied this metastability by performing molecular dynamics (MD) simulations [36] in which the pseudomorphic Ni/Ag(100) system is heated to elevated temperatures. The simulations were carried out at coverages of 3.13 and 4.70 ML of Ni, allowing two Ag layers to move in addition to the entire Ni film. Trajectories were 140 and 60 ps in length, respectively. At least for these short times, both the 3.13 and 4.70 ML films remained pseudomorphic all the way up to 1000 K. Thus the kinetic barrier to a collectively instigated phase transition appears quite high.

If incommensurate growth of a Ni thin film could occur in the first monolayer, one might expect to form either a Ni(100)/Ag(100) or a Ni(111)/Ag(100) interface. We performed MC simulations at 300 K in which one full atomic layer of each of these structures were equilibrated. Both the Ni(100) and Ni(111) structures are more densely packed than the Ag substrate. The number of atoms in each atomic layer corresponds to pseudomorphic coverages of 1.37 ML (280 Ni atoms) and 1.56 ML (320 Ni atoms) for Ni(100) and Ni(111), respectively. Both of these interfaces have large misfits with the substrate, resulting in regions where Ni atoms sit directly above substrate Ag atoms. As we see below, these dislocations dramatically affect the resulting interfacial structures.

The Ni(100) film was found to be unstable at 300 K. As mentioned above, an atop site location for Ni is high in energy. Therefore, it is not surprising that we find the atoms in the initial Ni(100) structure that lay directly above Ag substrate atoms get pushed up into second layer positions, leaving a pseudomorphic layer at the interface. The Ni(111) structure was found to be stable under similar conditions, but it is buckled at positions where Ni atoms rest close to atop sites (directly above substrate atoms). The most favorable orientation of the Ni(111) overlayer is to align the $[01\bar{1}]$ direction of the adlayer with the [001] direction of the substrate.

We also examined an equilibrated structure at 300 K for two Ni(111) adlayers (640 atoms). The first layer is buckled as in the monolayer case (amplitude ~ 0.5 Å) and buckling in the second layer away from the interface is only slightly attenuated (amplitude ~ 0.4 Å). Fig. 8a displays this buckling for a single Ni(111) layer that has been quenched to 0 K. The view in fig. 8b is along the substrate [001] direction and the wave is along the substrate [010] direction. Because we are looking across several rows of atoms, we see both the crests and troughs by scanning from left to right across the film shown in fig. 8a. The atoms that lie closest to the substrate layer are resting in pseudomorphic sites while those atoms pushed farthest away from the substrate are in atop sites, directly above substrate atoms. The node corresponds to a plane of Ni atoms that rest in neither atop nor pseudomorphic sites. The amplitude of the distortion perpendicular to the surface is ~ 0.6 Å for the Ni(111) layer and ~ 0.2 Å for the layer of Ag(100) closest to the surface. The buckling wavelengths of the Ni(111) layer in both the Ag[001] and Ag[010] directions are ~ 6 and ~ 72 Å, respectively. The buckling

pattern did not change when the periodic cell dimensions were changed by making it square (19×19) or increasing the longer dimension (to 38×6), indicating this is not an artifact of the simulation. These latter periodic dimensions also minimize the strain in the Ni(111) adlayer (0.76% for the 19×19 periodic cell and 0.10% and 1.45% for the 38×6 cell).

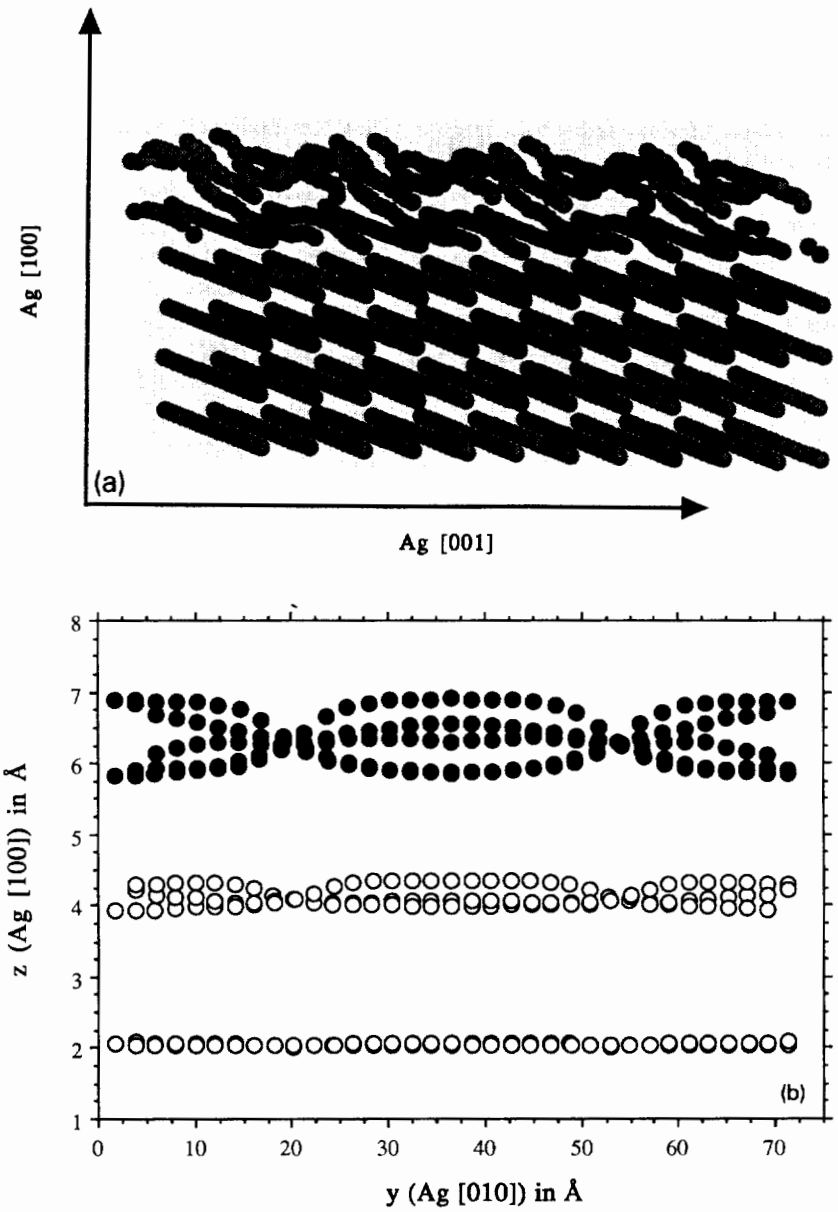

Fig. 8. (a) The 1 ML Ni(111)/Ag(100) minimum energy structure (at 0 K). The overlayer buckles with periodic waves in both the Ag[001] and Ag[010] directions. The view is from slightly above the Ag[010] direction. (b) The structure of the same Ni(111)/Ag(100) interface looking along a line parallel to both the Ag[001] and Ni[01$\bar{1}$] directions. Here the (○) represents Ag atoms and the (●) represents Ni atoms.

We have seen wave-like distortions in our earlier studies of fcc/bcc interfaces [22]. However, in those cases the distortions occurred in the plane of the overlayer rather than inducing buckling toward the vacuum. Misfit dislocations in the fcc/bcc interface could be relieved in this way because of the inherent asymmetry (or rectangular nature) of the bcc(110) substrate. However, the fcc(100) substrate has no such asymmetry, thus no preferential direction exists to distort the overlayer within the surface plane. Thus, buckling occurs perpendicular to the surface plane to relieve dislocations where atoms reside on top of other atoms. We are investigating whether such perpendicular and parallel mass density waves are a general phenomenon that can be systematically predicted if the symmetry and lattice mismatch of the substrate and adlayer are known [37].

3.5. Ni–Ag interdiffusion via exchange

Rh films grown on Ag(100) and Cu(100) have been observed to undergo substrate atom diffusion upon annealing to form a capping layer of the coinage metal above the thin film [26,27]. Ni has a smaller lattice constant than Rh ($a_0^{Ni} = 3.52$ Å compared with $a_0^{Rh} = 3.80$ Å), leading to a larger lattice strain for the Ni/Ag(100) system. This may inhibit exchange at a Ni(111)/Ag(100) interface due to the large distortion this exchange would cause in the Ni film. The surface energy of Ni is lower than Rh but still larger than Ag(100). This means that a driving force for Ag/Ni exchange still exists, although it is less than in the Rh/Ag case. If the Ni film grows pseudomorphically, the more open (100) structure is expected to have a lower barrier to interdiffusion than the close packed Ni(111) overlayer.

In order to investigate the possibility of Ag capping of the thin film, we performed MC simulations similar to the one mentioned above, except that every MC step there is a small probability (set to 0.004) that an exchange of a Ni and Ag atom pair will be attempted. Starting with a 3.43 ML pseudomorphic film formed by deposition, Ag did form a capping monolayer at 300 K. This did not disrupt the pseudomorphic nature of the Ni thin film and we observed no alloying. Since no interdiffusion of Ni occurred during the vapor deposition simulations (using a normal MC simulation without exchange), we conclude that there are two competing effects, one kinetic and the other thermodynamic. Thermodynamically, there is a large driving force for the formation of capping layers, especially for pseudomorphic Ni/Ag(100). Kinetically, this capping will involve diffusion through one or more layers of Ni and thus will not occur readily at low temperature or through thick films. Raeker, Sanders and Depristo observed interdiffusion in simulations of Rh/Ag(100) [19,20], but they only investigated Rh coverages of less than 1 ML.

We performed similar MC simulations with atom–atom exchange for the case of two layers of Ni(111) on Ag(100) to see if the more compact Ni(111) lattice would allow such exchange. We find that Ni/Ag exchange is so unfavorable that no Ag capping can occur. Thus the less-dense pseudomorphic Ni films allow a mechanism for exchange and thus favor formation of a Ag capping layer, while the close-packed Ni(111) does not. From the experimental work, it is not clear whether the structure of the "sandwiched" material is pseudomorphic [27,28], but these simulations indicate that a pseudomorphic Ni layer may be preferred.

4. Summary and conclusions

For submonolayer coverages of Ni grown on Ag(100), we find that Ni atoms adsorb near pseudomorphic lattice sites but with two-dimensional clustering of Ni atoms, which breaks the pseudomorphic symmetry. This phenomenon might be observable with LEED and appears to be an efficient means of relieving the homogeneous lateral strain present within the pseudomorphic Ni adlayer. Such clustering may be present in other fcc/fcc(100) systems where a large lattice strain exists.

As the film grows via vapor deposition at 300 K, pseudomorphic growth continues. The Ni–Ni nn bond distance decreases monotonically away from Ni/Ag interface (from 2.80 Å near the

interface to 2.60 Å close to the film's surface). The interlayer spacing is contracted relative to the bulk Ni interlayer spacing, in order to compensate for the lateral strain of Ni atoms within each atomic plane parallel to the interface. The resulting crystal structure is a tetragonal phase of Ni. As the coverage increases, the pseudomorphic film becomes thermodynamically unstable at approximately 3.0–3.3 ML (at 0 K). This result, that a pseudomorphic film is stable for a system with 13.9% lattice strain, suggests that previous predictions of an upper bound for such growth at 9–13% strain are not quite correct [1,6–12]. This discrepancy is primarily due to the neglect by prior models of atomic relaxation in the growing film. These relaxations allow contractions of the atomic spacings perpendicular to the plane of the surface, which compensate for lateral strain.

The pseudomorphic Ni film is also unstable with respect to formation of a "sandwich" Ag/Ni(pseudomorphic)/Ag(100) structure, created by interdiffusion of the Ag atoms. Since the surface free energy of Ag(100) is less than that of Ni(100), and certainly less than expansively strained Ni(100), a thermodynamic driving force exists to cap the Ni film with a monolayer of Ag. The more open structure of the Ni(100) film should also kinetically favor a sandwich structure. However, we caution that we have not found dynamical pathways for Ag diffusion through the Ni overlayer,hence there may be exceedingly large kinetic barriers to forming the capping Ag overlayer. Above 3.3 ML, a Ni(111) structure is predicted to be the most stable film at 0 K. Because of the misfit between Ni(111) and Ag(100), the Ni adlayer is buckled normal to the surface. The close-packed structure of the Ni(111) film is found to inhibit interdiffusion and formation of a capping Ag layer.

Acknowledgements

We wish to thank the Office of Naval Research (Grant No. H00014-89-J-1492) for support of this work. E.A.C. acknowledges support from the National Science Foundation and the Camille and Henry Dreyfus Foundation through their Presidential Young Investigator and Distinguished New Faculty Awards programs, respectively. We also wish to thank Professor R.S. Williams for several stimulating discussions. Simulations were performed on an FPS 521-EA computer obtained via the Department of Defense University Research Instrumentation Program (Grant No. H00014-89-J-1378).

References

[1] F.C. Frank and J.H. van der Merwe, Proc. R. Soc. A 200 (1949) 125.
[2] M. Smollet and M. Blackman, Proc. R. Soc. London A 64 (1951) 683.
[3] J.H. van der Merwe and M.W.H. Braun, Appl. Surf. Sci. 22/23 (1985) 545.
[4] E. Bauer and J.H. van der Merwe, Phys. Rev. B 33 (1986) 3657.
[5] F.C. Frank and J.H. van der Merwe, Proc. R. Soc. A 198 (1949) 205.
[6] I. Markov and A. Milchev, Surf. Sci. 136 (1984) 503.
[7] I. Markov and A. Milchev, Surf. Sci. 136 (1984) 519.
[8] I. Markov and A. Milchev, Surf. Sci. 145 (1984) 313.
[9] B.W. Dodson and P.A. Taylor, Phys. Rev. B 34 (1986) 2112.
[10] P.A. Taylor and B.W. Dodson, Phys. Rev. B 36 (1987) 1355.
[11] D.A. Faux, G. Gaynor, C.L. Carson, C.K. Hall and J. Bernholc, Phys. Rev. B 42 (1990) 2914.
[12] B.W. Dodson, Surf. Sci. 184 (1987) 1.
[13] A. Kobayashi and S. Das Sarma, Phys. Rev. B 35 (1987) 8042.
[14] A.S. Nandedkar, G.R. Srinivasan and C.S. Murthy, Phys. Rev. B 43 (1991) 7308.
[15] C.S. Murthy and B.M. Rice, Phys. Rev. B 41 (1990) 3391.
[16] The misfit is defined as $(a - b)/b$ where a is the lattice constant of the adlayer and b is the lattice constant of the substrate.
[17] R. Ramirez, A. Rahman and I.K. Schuller, Phys. Rev. B 30 (1984) 6208.
[18] S.M. Foiles, Surf. Sci. 191 (1987) 329.
[19] T.J. Raeker and A.E. DePristo, Surf. Sci. 248 (1991) 134 .
[20] T.J. Raeker, D.E. Sanders and A.E. DePristo, J. Vac. Sci. Technol. A 8 (1990) 3531 .
[21] B.C. Bolding and E.A. Carter, Phys. Rev. B 42 (1990) 11380.
[22] B.C. Bolding and E.A. Carter, Phys. Rev. B 44 (1991) 3251.
[23] A. Brodde, G. Wilhelmi, D. Bradt, H. Wengelnik and H. Neddermeyer, J. Vac. Sci. Technol. B 9 (1991) 920.
[24] R. Krishnan and M. Tessier, Solid State Commun. 60 (1986) 637.

[25] R. Krishnan and M. Tessier, Phys. Status Solidi (a) 97 (1986) K39.
[26] P.J. Schmitz, W.Y. Leung, G.W. Graham and P.A. Thiel, Phys. Rev. B 40 (1989) 11477.
[27] G.W. Graham, P.J. Schmitz and P.A. Thiel, Phys. Rev. B 41 (1990) 3353.
[28] S.J. Simko, Y. Cheng and M.C. Militello, J. Vac. Sci. Technol. A 9 (1991) 1477.
[29] S.M. Foiles, M.I. Baskes and M.S. Daw, Phys. Rev. B 33 (1986) 7983.
[30] M.S. Daw and M.I. Baskes, Phys. Rev. B 29 (1984) 6443.
[31] S.M. Foiles, Phys. Rev. B 32 (1985) 7685.
[32] B.W. Dodson, Surf. Sci. 184 (1987) 1.
[33] D. Wolf, Surf. Sci. 225 (1990) 117.
[34] P. Gumbsch, M.S. Daw, S.M. Foiles and H.F. Fischmeister, Phys. Rev. B 43 (1991) 13833.
[35] R.S. Williams, to be published.
[36] The molecular dynamics simulations were performed using the velocity form of the Verlet algorithm and using stochastic temperature control [H.C. Andersen, J. Chem. Phys. 72 (1980) 2384]. Rate-wise collisions were used to heat the system.
[37] B.C. Bolding, B.C. Hitz and E.A. Carter, to be published.